JACS
JOURNAL OF THE AMERICAN CHEMICAL SOCIETY
Article
pubs.acs.org/JACS

Membrane-Proximal Domain of a Disintegrin and Metalloprotease-17 Represents the Putative Molecular Switch of Its Shedding Activity Operated by Protein-disulfide Isomerase

Stefan Düsterhöft,[†,∥] Sascha Jung,[†,∥] Chien-Wen Hung,[‡,∥] Andreas Tholey,[‡] Frank D. Sönnichsen,[§] Joachim Grötzinger,*[,†] and Inken Lorenzen[†]

[†]Institute of Biochemistry, Christian-Albrechts-Universität zu Kiel, Olshausenstr. 40, 24098 Kiel, Germany

[‡]Institute for Experimental Medicine — Division of Systematic Proteome Research, Christian-Albrechts-Universität zu Kiel, Niemannsweg 11, 24105 Kiel, Germany

[§]Otto Diels Institute of Organic Chemistry, Christian-Albrechts-Universität zu Kiel, Olshausenstr. 40, 24098 Kiel, Germany

Supporting Information

ABSTRACT: A disintegrin and metalloprotease-17 (ADAM17) is a major sheddase responsible for the regulation of a wide range of biological processes, like cellular differentiation, regeneration, or cancer progression. Hitherto, the mechanism regulating the enzymatic activity of ADAM17 is poorly understood. Recently, protein-disulfide isomerase (PDI) was shown to interact with ADAM17 and to down-regulate its enzymatic activity. Here we demonstrate by NMR spectroscopy and tandem-mass spectrometry that PDI directly interacts with the membrane-proximal domain (MPD), a domain of ADAM17 involved in its dimerization and substrate recognition. PDI catalyzes an isomerization of disulfide bridges within the thioredoxin motif $C_{600}XXC_{603}$ of the MPD and results in a drastic structural change between an active open state and an inactive closed conformation. This conformational change of the MPD putatively acts as a molecular switch, facilitating a global reorientation of the extracellular domains in ADAM17 and regulating its shedding activity.

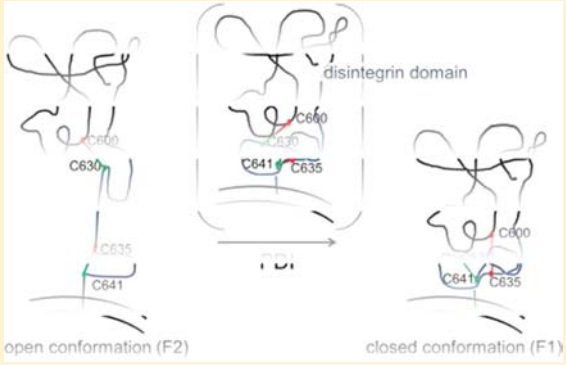

INTRODUCTION

ADAM17 (a disintegrin and metalloprotease-17) is a membrane-bound metalloprotease, also known as tumor necrosis factor-α converting enzyme (TACE). This enzyme is essential in developmental processes, as demonstrated by the perinatal lethality of ADAM17 knockout mice.[1] Moreover, investigation of conditional knockout mice[2] and hypomorphic ADAM17 knock-in mice[3] revealed that ADAM17 is a molecular switch in many immune responses, regeneration processes, and cancer development.

It proteolytically processes more than 75 substrates involved in many physiological events, like cell migration and proliferation.[4] Substrates include growth factors, adhesion molecules, pro-inflammatory cytokines, and cytokine receptors.[4] Thereby, the proteolytic process, also named shedding, constitutes a rapid irreversible regulatory switch as a response to different stimuli.

As type-I transmembrane multidomain proteins, ADAMs consist of an N-terminal signal peptide followed by a pro-, a metalloprotease-, a disintegrin-, a cysteine-rich-, and an EGF-like domain in the extracellular region, followed by a single transmembrane region and a cytoplasmic tail. ADAM17 and its closest relative ADAM10 are atypical members of the family, as a membrane-proximal domain (MPD) in their extracellular region replaces the cysteine-rich and EGF-like domains.[5,6] The structure and fold of this domain in ADAM17 is unknown and as of yet unclassified. Like the disintegrin domain with 16 cysteine residues, the MPD is rich in cysteine residues comprising 5 disulfide bonds, and its fold is expected to be governed by disulfide bonds.

ADAM10 is predominantly constitutively active, whereas ADAM17 is activated by a still unknown regulatory mechanism.[7,8] In a structural model,[5,9] the disintegrin domain acts as a scaffold that places its neighboring domains in a correct relative spatial position, placing the so-called hypervariable region of the MPD in close proximity to the active site of the enzyme.[9] This model places a central role on this domain since it is involved in substrate recognition, regulation, and multimerization of this enzyme,[5,9−17] without knowing details for regulatory interactions and possible structural changes.

Principally, a possible regulatory mechanism could target disulfide linkages in ADAM17. The protease was originally shown to be redox sensitive, being activated by H_2O_2 and inactivated by the addition of DTT.[13] This crude experiment was recently corroborated by the finding that cell-surface

Received: January 11, 2013
Published: March 22, 2013

dx.doi.org/10.1021/ja400340u | J. Am. Chem. Soc. 2013, 135, 5776−5781

protein-disulfide isomerase (PDI) is able to inactivate the enzyme[15] due to a conformational change within the noncatalytic extracellular part of ADAM17.[8,15] Furthermore, Bennet et al. showed that blocking of cell-surface PDI induces ADAM17 mediated L-selectin shedding.[18] We confirmed these findings by our own experiments using cells overexpressing ADAM17 as well as PDI (Supporting Information, Figure S1). Putative sites for PDI isomerization include two thioredoxin CXXC motifs present in the noncatalytic extracellular domain of ADAM17. While one of these is located in the disintegrin domain, particularly the second motif within the MPD is a likely candidate for thiol isomerization.

Li et al. identified one of these cysteine residues, C600, as crucial for the activity of the full-length ADAM17.[14] Additional findings revealed that also the mutation of both amino acid residues between the cysteine residues C600 and C603 of the thioredoxin motif of the MPD but not of the disintegrin domain lead to an inactive ADAM17 variant.[13] Members of the PDI family are oxidoreductases which are well-known to induce conformational changes within extracellular domains of membrane-bound proteins.[19−23] Its "classical" role is the rearrangement of disulfide linkages in the endoplasmic reticulum (ER), thereby promoting protein folding and stability.[22] In recent years, it was repeatedly described that the PDIs are also localized at the cell surface, playing important roles in various regulatory processes.[20−27] Since C600 in the thioredoxin motif of the MPD is crucial for ADAM17 activity,[13,14] we hypothesized that this domain represents the putative molecular switch of ADAM17 shedding activity mediated by the PDI. Here, we present the molecular consequences of a cysteine isomerization within the isolated MPD of human ADAM17 caused by PDI: A large structural change converts a less structured open form, corresponding to the active state of ADAM17, into a well-defined closed structure corresponding to the inactive state of ADAM17.

RESULTS

Expression, Purification, and Structural Characterization of the MPD of ADAM17. To analyze the molecular level of the PDI-mediated inactivation of ADAM17, we aimed to characterize the structure of the isolated domain. The cDNA of this domain was cloned into the bacterial expression vector. The *E. coli* expressed protein was soluble and was initially purified via its N-terminal His-tag. In a subsequent size-exclusion chromatography MPD eluted as a monomeric protein (Figure 1A). Surprisingly, a $^{1}H-^{15}N$-HSQC spectrum of this material displayed only a small number of well-resolved resonances (Figure S2, Supporting Information). As aggregation could be excluded, we concluded that multiple monomeric disulfide isomers existed in solution. Therefore, the NMR sample was analyzed by RP-HPLC. The protein eluted as two sharp (F1 and F2) and one broader peak (F3) (Figure 1B). Intact protein masses of fractions F1 and F2 were determined by HPLC ESI Orbitrap mass spectrometry (MS). The accurate masses of 9739.265 Da obtained for both forms (Figures S3A and S3B, Supporting Information) are in excellent agreement with the theoretical mass, calculated for the fully oxidized, disulfide-bonded protein.

$^{1}H-^{15}N$-HSQC spectra recorded of RP-HPLC fractions indicated that F3 contained only unfolded protein. Spectra of F1 and F2 are indicative of well-structured proteins, each in a single conformation (Figure 1C and D). The F1 spectrum approximately shows the expected number of resonance peaks.

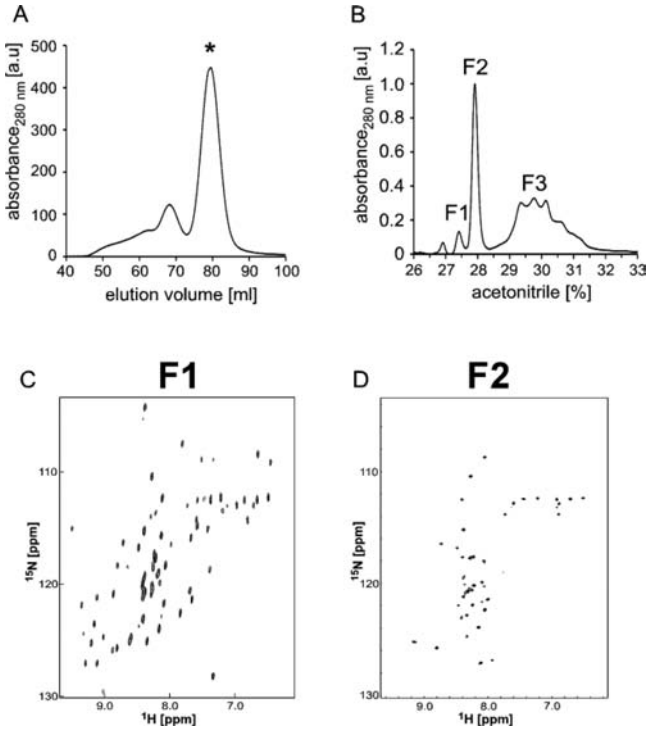

Figure 1. MPD of ADAM17 expressed in various disulfide-isomer conformations. (A) Ni-affinity purified MPD was applied to size-exclusion chromatography resulting in a major fraction containing the MPD in its monomeric state (*). (B) The monomeric MPD sample was loaded onto a RP-HPLC column equilibrated with 2% acetonitrile in H_2O/0.1% trifluoroacetic acid and eluted using a gradient from 2 to 95% (0.64% acetonitrile per minute). Only fractions containing the MPD protein are labeled; these include two well-separated peaks (F1 and F2) as well as a bulk of nonseparated peaks (F3). (C) The $^{1}H-^{15}N$-HSQC NMR spectrum of fraction F1 contained well-dispersed signals. (D) The $^{1}H-^{15}N$-HSQC NMR spectrum of fraction F2 contained also well-dispersed signals showing identical chemical shifts as F1, but the total number of resonances is much less compared to the spectrum of F1.

Interestingly, all resonances of F2 display nearly identical chemical shifts compared to F1, but the number of resonances is less. Several resonances are missing, presumably as a result of flexibility within the F2 isomer. Since F1 elutes at a lower acetonitrile concentration in the RP-HPLC, we concluded that this form might be less hydrophobic and more compact than F2. Accordingly, we named these two isoforms as closed (F1) and open (F2) conformation.

Structure of the Closed Conformation of the MPD of ADAM17. The structure of the closed conformation of the MPD (F1) was solved by heteronuclear NMR spectroscopy using a series of three-dimensional experiments (see Supporting Information). The statistics of the structure calculation are summarized in Table 1. The ensemble of the 20 energetically best structures and a representative structure is shown in Figure 2A and 2B, respectively. On the basis of secondary structure elements, the MPD of ADAM17 can be divided into two regions, a larger N-terminal and a smaller C-terminal region. The N-terminal region contains two small α-helices and a three-stranded antiparallel β-sheet, whereas the C-terminal region comprises a small three-stranded antiparallel β-sheet. The superposition of the MPD of ADAM17 with that of ADAM10[5] displays a high structural similarity of both domains (Figure 2C).

dx.doi.org/10.1021/ja400340u | J. Am. Chem. Soc. 2013, 135, 5776−5781

Table 1. Structural Statistics for the 20 Structures with the Lowest Energy

distance restraints	number
intraresidual ($\|i-j\|=0$)	131
sequential ($\|i-j\|=1$)	148
medium range ($2 \le \|i-j\| \le 4$)	47
long range ($\|i-j\| \ge 5$)	112
disulfide bonds (included)	30
total	438
deviation from idealized geometry	
bond length	0.0190 ± 0.0005 Å
bond angles	2.2413 ± 0.0496°
impropers	2.0916 ± 0.1507°
mean global backbone rmsd to mean[a]	0.62 ± 0.19 Å
mean global heavy rmsd to mean[a]	1.27 ± 0.18 Å
Ramachandran plot	
most favored regions	83.2%
additional allowed regions	16.4%
generously allowed regions	0.3%
disallowed regions	0.1%

[a]Residues considered: 8−35, 39−56, 59−61.

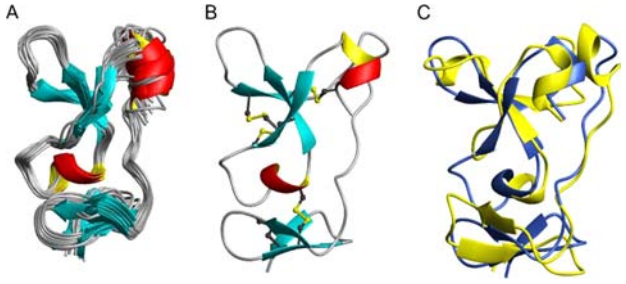

Figure 2. Structure of the closed MPD of ADAM17. (A) Ribbon representation of an ensemble of the 20 energetically best structures. (B) Ribbon representation of a representative structure of the MPD with disulfide bridges depicted as gray and yellow balls and sticks. (C) Superposition of the MPD of ADAM17 (blue) with those of its closest relative ADAM10 (yellow, pdb 2AO7[5]).

Structural Differences of the Open and Closed Conformers of the ADAM17 MPD. A complete structural characterization akin to the closed form was not possible for the open form due to the significant number of missing residues. An overlay of HSQC spectra for both forms illustrate that the open conformation (F2) displays about 32% fewer resonances than the closed one (Figure 3A). Nevertheless, the resonances that are present exhibit chemical shifts very similar to those of the closed MPD (F1). Their identity in the open form was partially confirmed by independent resonance and sequential assignment using a series of three-dimensional heteronuclear NMR spectra, which also proved that all missing amide resonances did indeed vanish presumably due to fast exchange and did not shift as one might alternatively expect.

Identical chemical shifts within the open and closed MPD for about 60% of residues indicate that the corresponding residues have a comparable chemical environment and, therefore, must adopt similar structures (Figure 3B). Especially, the six cysteine residues of the disulfide bonds C582−C604, C591−C611, and C593−C603 exhibit the same $^{1}H/^{15}N$ chemical shifts in both conformations, indicating their structural consistency in both conformers. This is further supported by the fact that in addition to their $^{1}H/^{15}N$ chemical shifts also the frequencies of their side-chain atoms are similar in both conformations. In contrast, resonances of the cysteine residues involved in the C-terminally located disulfide bonds C600−C635 and C630−C641 are absent in the open form. Further, all missing resonances locate to residues in the C-terminal portion of MPD or residues in the MPD that are in contact with the C-terminal region (Figure 3B).

In the closed MPD (F1), the C-terminal part is well structured and connected to the upper part by the disulfide bridge formed by cysteine residues C600 and C635. In clear contrast, resonances of amino acid residues of this region are not appearing in the spectrum of the open conformation (F2), illustrating its entire flexibility and movement partially independent from the N-terminal part. As additional residues around C600 (E595-K601) also vanished in the open conformation (F2), these data raised the question how the cysteine residues are paired within the open conformer (F2).

Assignment of the Disulfide Linkages of the Open and Closed Conformers by Mass Spectrometry. To assign the disulfide linkages in the closed and the open conformation, a combination of proteolytic digestions and MS/MS experiments were used. The direct digestion of the nonreduced MPD with either trypsin or GluC-protease only delivered peptides not suitable for the assignment of disulfides; the peptides formed were either too long for straightforward MS/MS fragmentation or contained more than one disulfide, preventing unambiguous assignment. To increase the accessibility of proteolytic sites of the MPD, we developed and applied a modified solid-phase-based method[28] to partially reduce disulfide bonds in the separated protein isoforms under controlled conditions. The newly formed reduced cysteine residues were protected by rapid alkylation to prevent disulfide rearrangement. Intact protein LC−MS analysis of proteins showed a number of different reduced/alkylated species including fully reduced alkylated forms as well as species with one to four reduced disulfides (Figure S4, Supporting Information).

These proteins were subjected to proteolytic cleavage using both trypsin and Glu-C, and the resulting peptides were analyzed by nano-LC−ESI Orbitrap MS/MS. Two types of collision activation, collision-induced dissociation (CID) and high-energy collision dissociation (HCD), were applied to interrogate the peptide sequences and to assign disulfide linkage(s). Five disulfide linkages of the closed conformation were unambiguously identified: C582−C604, C591−C611, C593−C603, C600−C635, and C630−C641 (Tables S1 and S2, Supporting Information). These match the NMR data perfectly. For the open conformation, three disulfide bonds could be assigned: C591−C611, C600−C630, and C635−C641.

In summary, the open and the closed conformation are diverse with respect to their disulfide linkages in the C-terminal part, which can be readily recognized from their MS/MS spectra (Figure S5, Supporting Information). C582−C604, C591−C611, and C593−603 are present in both conformers. The thiol isomerization involves the disulfide bond that connects the N-terminal with the C-terminal part in the closed conformer (C600−C635). In the open conformation, C600 binds to C630 of the C-terminal part, accompanied by an isomerization of C630−C641 to C635−C641 (Figure 3C).

Protein Disulfide Isomerase Induced a Conformational Change within the MPD of ADAM17. Since PDI is supposed to inactivate ADAM17 by disulfide shuffling, resulting

dx.doi.org/10.1021/ja400340u | J. Am. Chem. Soc. 2013, 135, 5776−5781

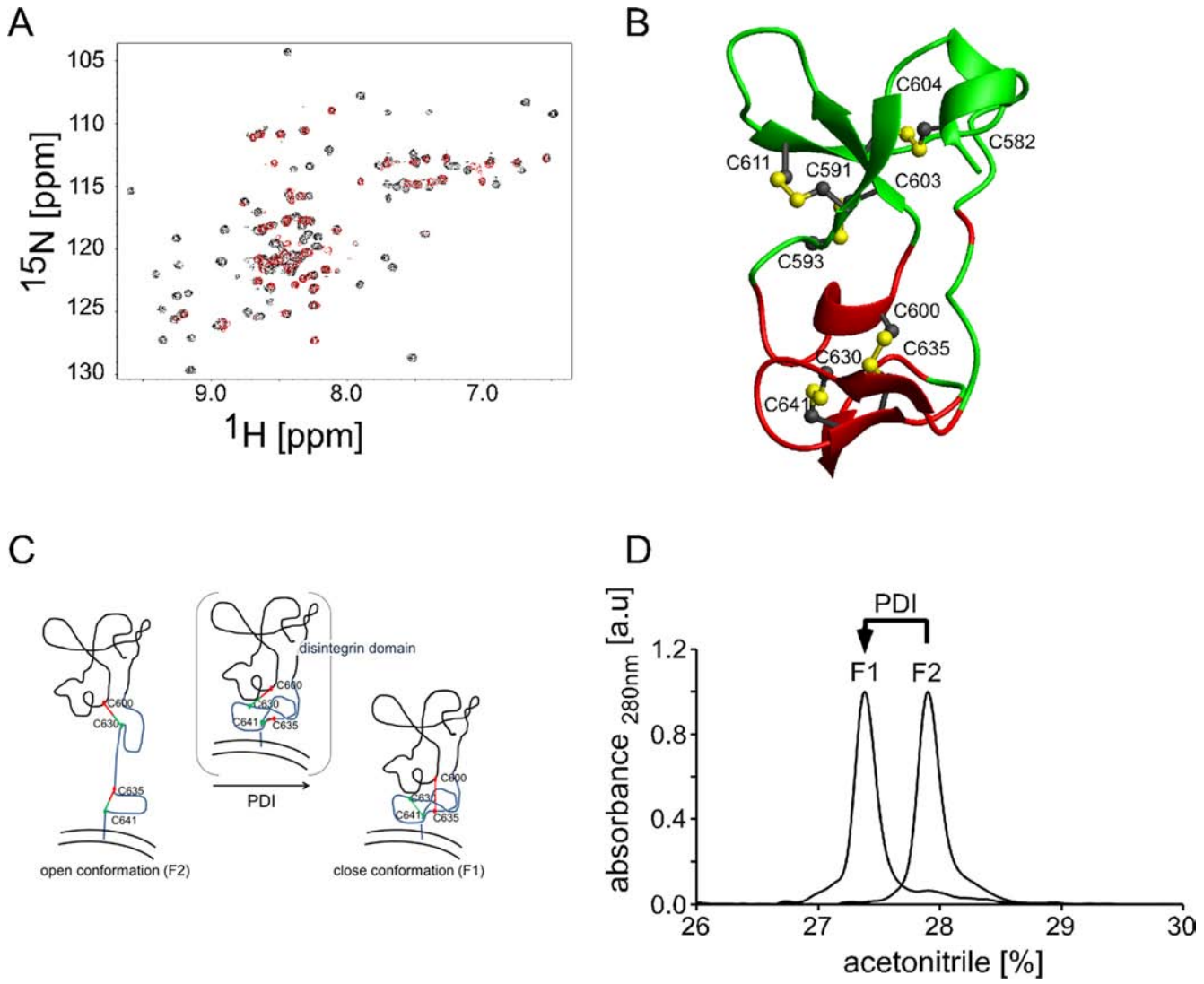

Figure 3. Structural differences of the open and closed conformation of the MPD. (A) Superposition of the $^{1}H-^{15}N$-HSQC spectra of both conformers. Resonances of the open conformer (F2, red) are located at identical chemical shifts like the corresponding ones of the closed isoform (F1, black). (B) Structure of the closed conformation of the MPD with disulfide bridges depicted as gray and yellow balls and sticks. Cysteine residues are labeled according to their absolute position in the primary structure of the full-length ADAM17. Backbone resonances that are structurally conserved, i.e., that are present in the HSQC spectra of both conformers (581−588, 590−594, 602−612, 614−621, 623−626, 638), are depicted in green, whereas backbone resonances that were not observable in the open conformer (595, 598−601, 622, 627, 628, 630−637, 639−642) are depicted in red. (C) Schematic presentation of the putative structural consequences of the PDI-mediated disulfide isomerization. (D) PDI-mediated conversion of the open conformation (F2) into the closed one (F1) analyzed by RP-HPLC.

in a conformational change within the protease, the influence of the PDI on the two conformers (F1 and F2) was analyzed by RP-HLPC. While an incubation of the open conformer (F2) with oxidized PDI does not change the elution profile of this domain, treatment with reduced PDI induced a change within this domain. Remarkably, the open conformer (F2) is shifted to the position of the closed MPD (F1) (Figure 3D). A $^{1}H-^{15}N$-HSQC NMR spectrum recorded with the PDI-converted domain perfectly superimposed with the one of the closed conformer (F1) revealing that all resonances had identical chemical shifts. These results clearly demonstrate that the PDI is able to convert the open conformer of the MPD to the closed one. In addition, this effect is specific for the open conformer. Neither the PDI in its oxidized nor in its reduced form induced a structural change within the closed conformation.

DISCUSSION

Beside its classical function within the ER, the PDI has been described to act also on the cell surface by catalyzing the isomerization of disulfide bonds within cell surface proteins.[19−22] As a consequence, proteins change their conformation resulting in a switch of their functional properties, including their activation or accessibility to proteolysis.[19−22] The PDI is tethered to the cell surface by interaction with either soluble "adapter" proteins like galectin-9[23] or transmembrane proteins like β3-integrin.[26] Similar to β3-integrin, ADAM17 is known to interact with the PDI.[15] In contrast to the integrins which are activated by the PDI,[19,20,22] ADAM17 is inactivated.[15−18]

On the basis of the prior findings that cell-surface localized PDI affects the disulfide-bond-rich, noncatalytic extracellular part of ADAM17,[15] and that in particular residue C600 within

dx.doi.org/10.1021/ja400340u | J. Am. Chem. Soc. 2013, 135, 5776−5781

the thioredoxin motif of the MPD[13,14] is required for the activity of ADAM17, we focused our study on this domain. Recombinant expression of the MPD yielded two distinct folded species divergent in their disulfide linkages. Through treatment with PDI the second conformer (F2) is transformed into the first conformer (F1). Interestingly, this conformer possesses a well-defined, three-dimensional structure and corresponds to the inactive state of ADAM17. The second conformer (F2) is only partially folded, is obtained exclusively directly after purification, and corresponds to the active state. All attempts to convert the closed (F1) conformer into the open (F2) MPD by treatment with DTT, H_2O_2, and reduced and oxidized glutathione in combination with or without oxidized and reduced human thioredoxin-1 were unsuccessful. The conversion from F2 into F1 was only achieved through addition of PDI. In this case, isomerization is fast and complete within minutes. Attempts to follow the conversion by NMR spectroscopy failed, as even at lowered temperature the reaction was completed within the preparation time of sample and instrument.

Before treatment with PDI, the extracellular part of the active protease is supposed to be elongated and flexible, adopting conformations allowing the enzyme to shed substrates in close proximity to the plasma membrane. This property seems to be fulfilled in the open conformer (F2) of the MPD, which lacks the structured β-stranded C-terminal part and is envisioned to possess an elongated, flexible stalk region. Treatment with PDI converts the open, active conformer (F2) into the closed, inactive one (F1). The stalk region compacts into a folded structure, including the C-terminal β-strands. This structural organization significantly limits the conformational freedom in the entire extracellular part of ADAM17 and putatively abolishes cleavage of substrates due to the inaccessibility of the cleavage sites for the catalytic domain.

Since the MPD was described to be involved in substrate recognition,[5,10,11] the proposed conformational change might also affect substrate recognition. The hypervariable region which is supposed to be involved in substrate recognition[9] is located in the upper conserved part of the molecule (R605-N621), adjacent to the cysteine residue C600. The structure of the hypervariable region is not directly affected by the PDI-mediated conformational change (Figure 3B). Hence, an altered substrate recognition is more likely due to a change in the overall orientation of the extracellular part of ADAM17, rather than to an alteration within the proposed binding epitope. To shed light on the structural consequences of this conformational change within the MPD onto the whole ADAM17, the structure determination of the full-length molecule in its active and inactive form would be of great benefit.

The closest relative of ADAM17 is ADAM10 which is a constitutively active protease, whereas ADAM17 has to be activated. The comparison of the structure of their MPDs revealed a high similarity. In future investigations it will be interesting to analyze if the MPD of ADAM10 also exists in two conformations, which are convertible by the PDI, or if this property is exclusively present in ADAM17, where it directly links this conformational change to the functional regulation of this important proteolytic enzyme.

CONCLUSION

ADAM17 is a highly regulated membrane-bound enzyme involved in many pathophysiological processes. In this work we analyzed a conformational change regulating the activity of this enzyme that is mediated by the PDI. A disulfide isomerization in the membrane-proximal domain of ADAM17 converts this domain from an open conformation into a closed one, thereby switching off the shedding activity of ADAM17.

EXPERIMENTAL SECTION

Expression and Purification. For bacterial expression the cDNA of the human MPD (amino acid residues F581 to E642) was cloned into pET28 (Merck, Darmstadt, Germany) and transformed into *E. coli* strain BL21.[29] The soluble expressed domain was purified in PBS by its N-terminal His-tag using a HisTrap HP-column (GE Healthcare, Munich, Germany). After elution using imidazole/PBS the protein was separated by size-exclusion chromatography (HiLoad 16/60 Superdex 75, GE Healthcare, Munich, Germany), as well as RP-HPLC (MultoHigh 100 RP, CS-Chromatography Service GmbH, Langerwehe, Germany). Finally the protein samples were lyophilized and dissolved in PBS.

Protein-disulfide Assay. To test whether PDI is able to structurally convert the MPD, PDI (TAKARA BIO, Japan) was used either in its reduced or in its oxidized form. To reduce the enzyme, 74 μM PDI was incubated with 40 mM DTT in PBS pH 7.4 at 4 °C for 14 h. Afterward DTT was removed, and 85 μM of the MPD was incubated with 6.5 μM PDI. The samples were analyzed and purified by RP-HPLC as described above.

NMR Spectroscopy. For structure determination by NMR spectroscopy, the MPD was labeled with ^{15}N- and ^{13}C-isotopes by expression in minimal media and purified as described for the nonlabeled material. All spectra were processed with NMRPipe[30] and analyzed with NMRViewJ.[31] Detailed information is given in the Supporting Information.

Structure Calculation. Structure calculations were performed using the program CYANA.[32] The structure calculation was based on 609 interproton distances derived from ^{15}N- and ^{13}C-edited three-dimensional NOESY experiments. Distance restraints were calibrated using an r^6 function. Five disulfide bonds were defined as 15 distance restraint ranges as follows: $2.0 \le d(S_i^{\gamma}, S_j^{\gamma}) \le 2.1$ Å; $3.0 \le d(C_i^{\beta}, S_j^{\gamma}) \le 3.1$ Å; $3.0 \le d(S_i^{\gamma}, C_j^{\beta},) \le 3.1$ Å. TALOS+[33,34] was used for deriving backbone torsion angles from the NMR chemical shifts of the MPD and included in the structure calculations. One hundred structures were calculated and subsequently refined in explicit solvent with the CNS program using the RECOORD protocol and parameters.[35] The 20 energetically best structures with an NOE violation energy below a cutoff were selected as the final refined structural ensemble and were deposited (protein data bank accession code: 2m2f). All molecular graphical representations were generated using the programs MOLMOL.[36]

Assignment of Disulfide Bridges by Mass Spectrometry. Assignment of disulfide bonds was performed applying a partial reduction and alkylation strategy using a modified solid-phase-based method.[28] After proteolytic digestion either with single proteases or by applying sequential proteolytic digestions the resulting peptides were analyzed by LC-MS/MS on an LTQ Orbitrap Velos mass spectrometer (Thermo Fisher Scientific, Bremen, Germany). The interpretation of the data including the assignment of the disulfide bonds was performed manually. A detailed description is given in the Supporting Information.

ASSOCIATED CONTENT

Supporting Information

A more detailed description of the mass spectrometry and structure determination by NMR spectroscopy as well as cell based shedding assay. This material is available free of charge via the Internet at http://pubs.acs.org.

AUTHOR INFORMATION

Corresponding Author

jgroetzinger@biochem.uni-kiel.de

Author Contributions

[‖]These authors contributed equally.

Notes

The authors declare no competing financial interest.

■ ACKNOWLEDGMENTS

This study was supported by the Deutsche Forschungsgemeinschaft (SFB 877, A6, Z2 and Z3) and the Excellence Cluster 306 'Inflammation at Interfaces'. The authors would like to thank Sina Viehweg for their excellent technical assistance and Verena Pawlak for the help with the sequential assignment.

■ REFERENCES

(1) Peschon, J. J.; Slack, J. L.; Reddy, P.; Stocking, K. L.; Sunnarborg, S. W.; Lee, D. C.; Russell, W. E.; Castner, B. J.; Johnson, R. S.; Fitzner, J. N.; Boyce, R. W.; Nelson, N.; Kozlosky, C. J.; Wolfson, M. F.; Rauch, C. T.; Cerretti, D. P.; Paxton, R. J.; March, C. J.; Black, R. A. *Science* **1998**, *282*, 1281.

(2) Horiuchi, K.; Kimura, T.; Miyamoto, T.; Takaishi, H.; Okada, Y.; Toyama, Y.; Blobel, C. P. *J. Immunol.* **2007**, *179*, 2686.

(3) Chalaris, A.; Adam, N.; Sina, C.; Rosenstiel, P.; Lehmann-Koch, J.; Schirmacher, P.; Hartmann, D.; Cichy, J.; Gavrilova, O.; Schreiber, S.; Jostock, T.; Matthews, V.; Hasler, R.; Becker, C.; Neurath, M. F.; Reiss, K.; Saftig, P.; Scheller, J.; Rose-John, S. *J. Exp. Med.* **2010**, *207*, 1617.

(4) Scheller, J.; Chalaris, A.; Garbers, C.; Rose-John, S. *Trends Immunol.* **2011**, *32*, 380.

(5) Janes, P. W.; Saha, N.; Barton, W. A.; Kolev, M. V.; Wimmer-Kleikamp, S. H.; Nievergall, E.; Blobel, C. P.; Himanen, J. P.; Lackmann, M.; Nikolov, D. B. *Cell* **2005**, *123*, 291.

(6) Takeda, S. *Semin. Cell Dev. Biol.* **2009**, *20*, 146.

(7) Le Gall, S. M.; Bobé, P.; Reiss, K.; Horiuchi, K.; Niu, X. D.; Lundell, D.; Gibb, D. R.; Conrad, D.; Saftig, P.; Blobel, C. P. *Mol. Biol. Cell* **2009**, *20*, 1785.

(8) Le Gall, S. M.; Maretzky, T.; Issuree, P. D.; Niu, X. D.; Reiss, K.; Saftig, P.; Khokha, R.; Lundell, D.; Blobel, C. P. *J. Cell Sci.* **2010**, *123*, 3913.

(9) Takeda, S.; Igarashi, T.; Mori, H.; Araki, S. *EMBO J.* **2006**, *25*, 2388.

(10) Reddy, P.; Slack, J. L.; Davis, R.; Cerretti, D. P.; Kozlosky, C. J.; Blanton, R. A.; Shows, D.; Peschon, J. J.; Black, R. A. *J. Biol. Chem.* **2000**, *275*, 14608.

(11) Lorenzen, I.; Lokau, J.; Düsterhoft, S.; Trad, A.; Garbers, C.; Scheller, J.; Rose-John, S.; Grötzinger, J. *FEBS Lett.* **2012**, *586*, 1093.

(12) Milla, M. E.; Leesnitzer, M. A.; Moss, M. L.; Clay, W. C.; Carter, H. L.; Miller, A. B.; Su, J. L.; Lambert, M. H.; Willard, D. H.; Sheeley, D. M.; Kost, T. A.; Burkhart, W.; Moyer, M.; Blackburn, R. K.; Pahel, G. L.; Mitchell, J. L.; Hoffman, C. R.; Becherer, J. D. *J. Biol. Chem.* **1999**, *274*, 30563.

(13) Wang, Y.; Herrera, A. H.; Li, Y.; Belani, K. K.; Walcheck, B. *J. Immunol.* **2009**, *182*, 2449.

(14) Li, X.; Fan, H. *J. Biol. Chem.* **2004**, *279*, 27365.

(15) Willems, S. H.; Tape, C. J.; Stanley, P. L.; Taylor, N. A.; Mills, I. G.; Neal, D. E.; McCafferty, J.; Murphy, G. *Biochem. J.* **2010**, *428*, 439.

(16) Tape, C. J.; Willems, S. H.; Dombernowsky, S. L.; Stanley, P. L.; Fogarasi, M.; Ouwehand, W.; McCafferty, J.; Murphy, G. *Proc. Natl. Acad. Sci. U.S.A.* **2011**, *108*, 5578.

(17) Lorenzen, I.; Trad, A.; Grötzinger, J. *Biochem. Biophys. Res. Commun.* **2011**, *415*, 330.

(18) Bennett, T. A.; Edwards, B. S.; Sklar, L. A.; Rogelj, S. *J. Immunol.* **2000**, *164*, 4120.

(19) Lahav, J.; Gofer-Dadosh, N.; Luboshitz, J.; Hess, O.; Shaklai, M. *FEBS Lett.* **2000**, *475*, 89.

(20) Jordan, P. A.; Gibbins, J. M. *Antioxid. Redox Signaling* **2006**, *8*, 312.

(21) Kaiser, B. K.; Yim, D.; Chow, I. T.; Gonzalez, S.; Dai, Z.; Mann, H. H.; Strong, R. K.; Groh, V.; Spies, T. *Nature* **2007**, *447*, 482.

(22) Laurindo, F. R.; Pescatore, L. A.; Fernandes Dde, C. *Free Radical Biol. Med.* **2012**, *52*, 1954.

(23) Bi, S.; Hong, P. W.; Lee, B.; Baum, L. G. *Proc. Natl. Acad. Sci. U.S.A.* **2011**, *108*, 10650.

(24) Xiao, G.; Chung, T. F.; Pyun, H. Y.; Fine, R. E.; Johnson, R. J. *Brain Res. Mol. Brain Res.* **1999**, *72*, 121.

(25) Swiatkowska, M.; Szymanski, J.; Padula, G.; Cierniewski, C. S. *FEBS J.* **2008**, *275*, 1813.

(26) Cho, J.; Kennedy, D. R.; Lin, L.; Huang, M.; Merrill-Skoloff, G.; Furie, B. C.; Furie, B. *Blood* **2012**, *120*, 647.

(27) Söderberg, A.; Hossain, A.; Rosen, A. *Antioxid. Redox Signaling* **2013**, *16*, 363.

(28) Michalek, M.; Sönnichsen, F. D.; Wechselberger, R.; Dingley, A. J.; Hung, C. W.; Kopp, A.; Wienk, H.; Simanski, M.; Herbst, R.; Lorenzen, I.; Marciano-Cabral, F.; Gelhaus, C.; Gutsmann, T.; Tholey, A.; Grötzinger, J.; Leippe, M. *Nat. Chem. Biol.* **2013**, *9*, 37.

(29) Trad, A.; Hansen, H. P.; Shomali, M.; Peipp, M.; Klausz, K.; Hedemann, N.; Yamamoto, K.; Mauermann, A.; Desel, C.; Lorenzen, I.; Lemke, H.; Rose-John, S.; Grötzinger, J. *Cancer Immunol. Immunother.* **2013**, *62*, 411.

(30) Delaglio, F.; Grzesiek, S.; Vuister, G. W.; Zhu, G.; Pfeifer, J.; Bax, A. *J. Biomol. NMR* **1995**, *6*, 277.

(31) Johnson, B. A.; Blevins, R. A. *J. Biomol. NMR* **1994**, *4*, 603.

(32) Güntert, P. *Methods Mol. Biol.* **2004**, *278*, 353.

(33) Cornilescu, G.; Delaglio, F.; Bax, A. *J Biomol NMR* **1999**, *13*, 289.

(34) Shen, Y.; Delaglio, F.; Cornilescu, G.; Bax, A. *J Biomol NMR* **2009**, *44*, 213.

(35) Brünger, A. T.; Adams, P. D.; Clore, G. M.; DeLano, W. L.; Gros, P.; Grosse-Kunstleve, R. W.; Jiang, J. S.; Kuszewski, J.; Nilges, M.; Pannu, N. S.; Read, R. J.; Rice, L. M.; Simonson, T.; Warren, G. L. *Acta Crystallogr D Biol Crystallogr* **1998**, *54*, 905.

(36) Koradi, R.; Billeter, M.; Wüthrich, K. *J Mol Graph* **1996**, *14*, 51.